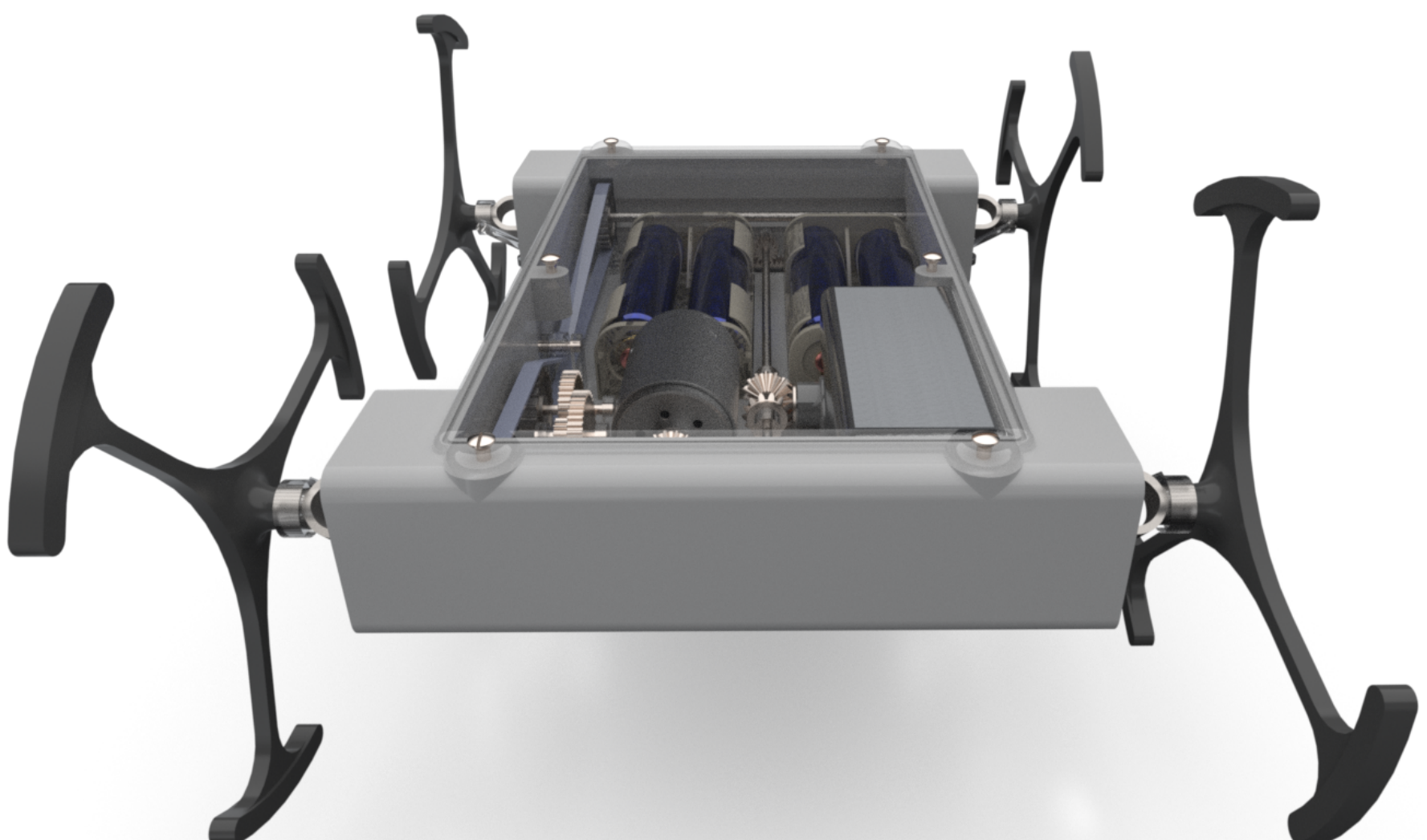


# MINIWHEG

**IMPERIAL COLLEGE  
DYSON SCHOOL OF DESIGN ENGINEERING  
GIZMO - PHYSICAL COMPUTING**

Alex Gibson - 01506897  
Spring Term 2020



# Table of contents

<b>Abstract</b>	2
<b>Nomenclature and abbreviations</b>	2
<b>1.0 Introduction</b>	3
<b>2.0 Research and Inspiration</b>	3
<b>3.0 Initial Design</b>	4
<b>4.0 Development and Iterations - Synthesis</b>	5
<b>4.1 Steering</b>	5
4.1.1 Servo and Gears	
4.1.2 Rack and Pinion	
<b>4.2 Motor Drive</b>	7
4.2.1 Motor	
4.2.2 Gearbox	
4.2.3 Power Transmission	
<b>4.3 Whegs</b>	9
4.3.1 Shape Iterations	
<b>4.4 Main body - Shell</b>	9
4.4.1 Shape Iterations	
4.4.2 Ingress Protection	
<b>5.0 Engineering Analysis - Analysis</b>	11
<b>5.1 Whег</b>	11
<b>5.2 Steering</b>	12
<b>6.0 Final Design</b>	13
<b>7.0 Renders</b>	14
<b>8.0 References</b>	15

# Abstract

This report outlines the design process of a miniature robot that moves using 'whegs' as opposed to traditional wheels. These whegs consist of 3 legs each which rotate 60° out of phase - a motion used by insects - allowing the robot to move at great speeds and overcome obstacles larger than the radius of the wh eg.

Having carried out research, it was discovered that these robots are used primarily to access areas which would otherwise be difficult due to rough terrain or size restrictions. It was therefore decided that the robot designed in this report would not only meet the specifications of the brief, but have improved capabilities for tackling such problems. Specifically, decreasing the radius of the turning circle was prioritised to allow for greater mobility in tight spaces.

After initial designs were explored and ideated, each of the components and mechanisms were iterated a number of times separately in SolidWorks to ensure functionality, and the final model was iterated and optimised so that all components worked in cohesion.

The final model had a length of 126.12 mm and a width of 88.50 mm, and weighed 154.76 grams. Whilst the length was well within the parameters specified by the brief, the width was larger. This was due to the focus placed on reducing the turning circle, and was deemed a necessary sacrifice for the added functionality. The final robot met all other specifications.

# Nomenclature and abbreviations

C <sub>2</sub>		Load factor
C <sub>3</sub>		Acceleration factor
C <sub>4</sub>		Fatigue factor
C <sub>0</sub>		Overall service factor
d	mm	Distance
D	m	Wh eg diameter
F	N	Tractive force
g	m/s <sup>2</sup>	Acceleration due to gravity
h	m	Height of obstacle
i		Speed ratio
m	kg	Mass of robot
n	rpm	Speed of gear
N		No. of teeth on gear
P	W	power
R	mm	Radius of wh eg
T	Nm	torque
v	m/s	Velocity
W	Nm	Work done
Z <sub>g</sub>	mm	No. of teeth of large toothed pulley
Z <sub>k</sub>	mm	No. of teeth of small toothed pulley
d <sub>wk</sub>	mm	Pitch diameter of small toothed pulley
d <sub>wg</sub>	mm	Pitch diameter of large toothed pulley
ω	rad/s	Rotational velocity

# 1.0 Introduction

'Miniwheg' describes a biologically inspired robot that uses spoked rotating axles to move in the place of wheels, moving in a similar fashion to an insect. They are optimised to overcome obstacles and traverse uneven terrain without difficulty and with a greater speed than would be possible with traditional wheels. The robots are primarily used to access cramped areas where a larger body could not fit, and to traverse surfaces such as extraterrestrial landscapes.

This report outlines the design process that led to the creation of a Miniwheg robot that fit within the parameters shown in the table to the right, which ensure the robots ability to perform the above tasks. Furthermore, a Miniwheg with as tight a turning circle as possible was created - this specific parameter was enhanced beyond the specification of the brief, as a tighter turning circle could help the Miniwheg achieve its real world tasks (such as search and rescue) more effectively, and with greater reliability - the ability to spin on its axis, for example, would prove invaluable.

Parameters	Specification
Length	≤ 160 mm
Width	≤ 80 mm
Weight	≤ 200 g
BoM Cost	≤ £100
Leg length	≤ 40 mm
Turning circle	≤ 160 mm
Payload	≥ 200 g
Speed	≥ 0.5 m/s
Drop height	≥ 300 mm
Climb obstacle	≥ 55 mm high
Electronics package	45 x 20 x 10 mm
Ingress protection	IP 53

**Table 1.** Miniwheg parameters and specifications

# 2.0 Research and Inspiration

Research was conducted into current designs of miniature biologically derived robots and mechanisms, in order to draw inspiration from the success of past and ongoing projects, and also to uncover where improvements could be implemented.

The main project that was looked into was the "Highly mobile and Robust Small Quadruped Robot" project<sup>1</sup>, led by the Biologically Inspired Robotics Lab at Case Western Reserve University. Many of the features of the MiniWheg designed during this project are interesting and implemented effectively, but also allow for refinement and enhancement. For example: the steering mechanism used only rotated the front whegs, meaning that the radius of the possible turning circle of the robot was limited - this could be improved by implementing a system that turns both sets of wheels simultaneously.

More in-depth research was conducted into the shape, orientation and design of the whegs. Research suggested that 3 spokes 120° apart and orientated 60° from each other is the most efficient arrangement, both for forward motion, and for overcoming obstacles.

Below are some examples I found of biologically inspired wheel design:

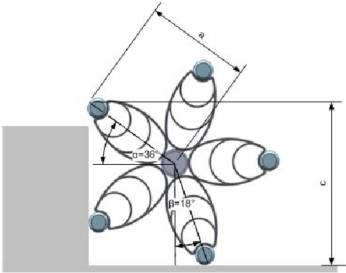
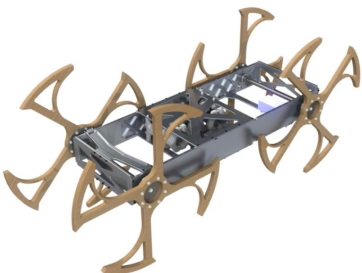
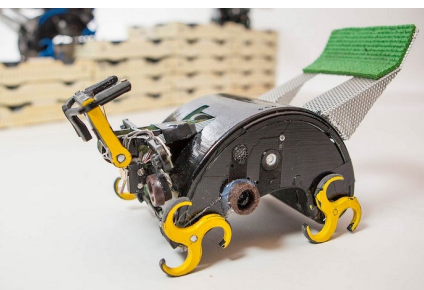


**Figure 1.** MiniWhegs IV robot designed by the Biologically Inspired Robotics Lab at Case Western Reserve University<sup>1</sup>

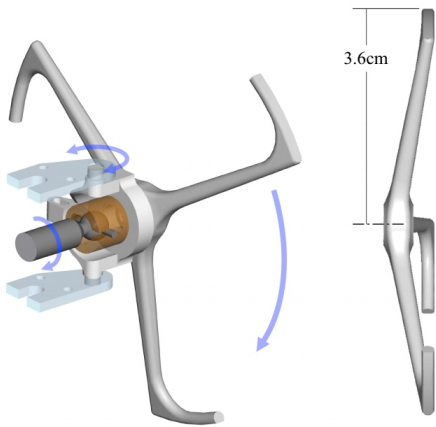


**Figure 2.** Turning mechanism of the Miniwheg IV robot<sup>1</sup>

**Figure 3.** Inspiration for wheel design, with 3<sup>3</sup>, 4<sup>4</sup> and 5<sup>2</sup> whegs



## 3.0 Initial Design

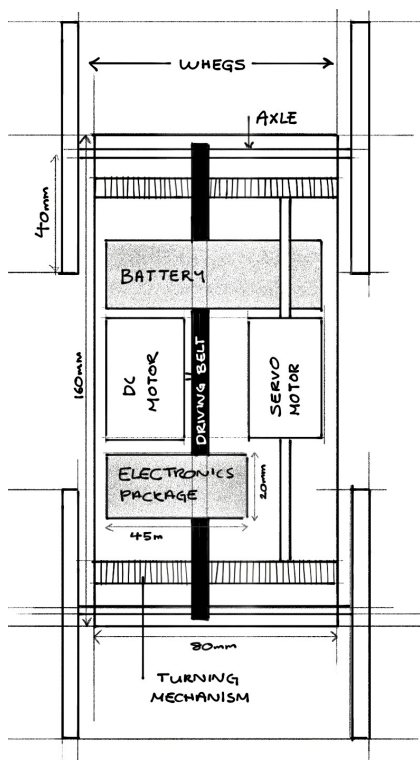


**Figure 4.** Potential layout of all components.

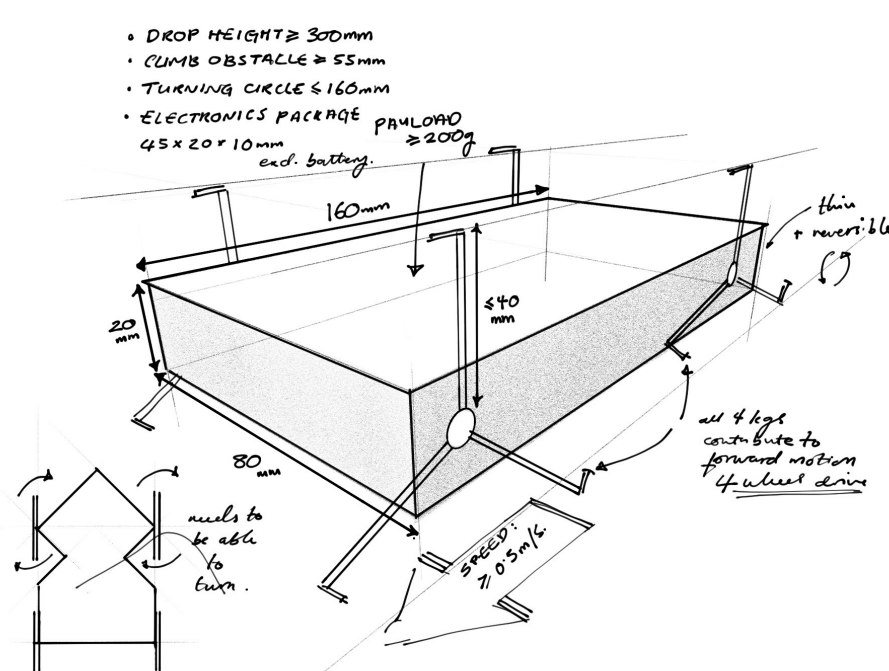


**Figure 5.** Simplified visual representation of the parameters and their specifications.

The design process was initiated by analysing the parameters that had been set for the robot and then creating simple sketches that visualised the basic layout and dimensions of parts. This was done as a first step to ensure that the parameters were known for any design iterations that were made, and all iterations were made within the specification of the brief.

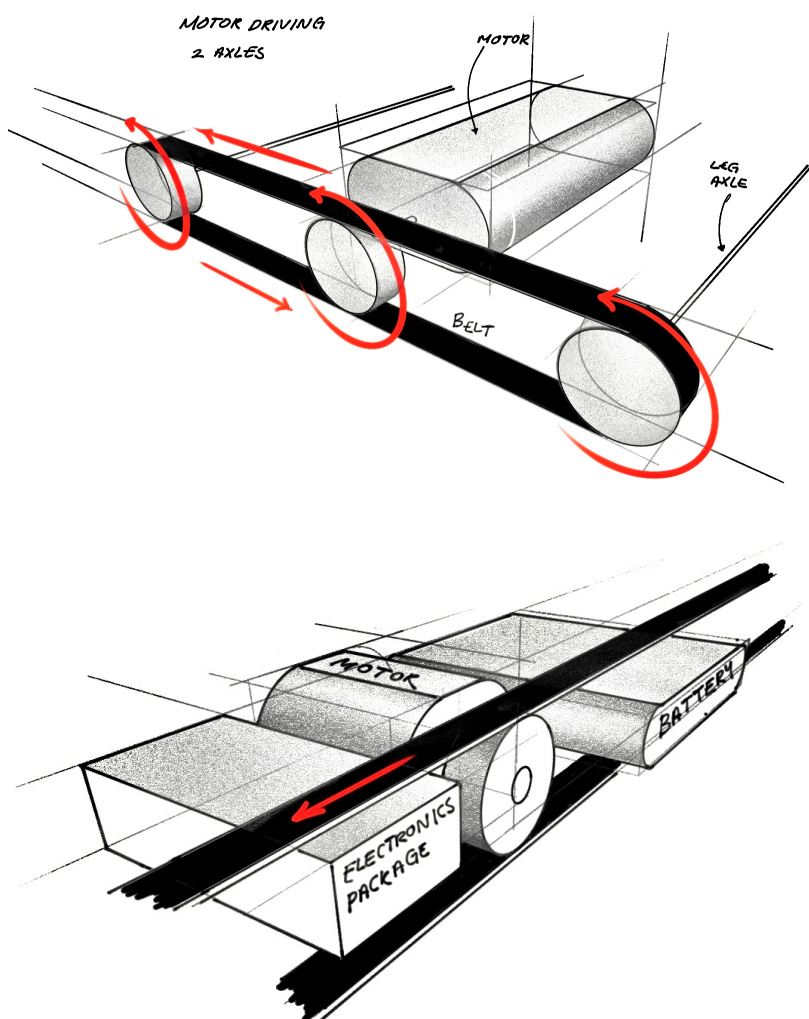


**Figure 6.** Exploring function of parts, and their potential configuration.

Having looked at the parameters, initial designs for individual parts were considered, as well as the functional requirements of the separate parts and how they would work in conjunction and close proximity. For example, using a belt to drive both axles simultaneously was considered (shown left), and ideas were sketched out to more easily visualise the components.

The configuration of parts needs to be considered from an early stage in the design process, as the transfer of power (for example from the motor to the axles) has the potential to take up a lot of valuable space within the robot. One idea is shown to the left, where the belt moves around the other components.

The design focus was also specified at this stage, and ideas were brainstormed for how to improve the function of the MiniWheg - it was decided that decreasing the radius of the turning circle would be the most advantageous improvement for traversing rough terrain and completing search missions. Designs to make this possible were then investigated and explored, moving the design phase into iterative and developmental ideation to realise these improvements.

N.B. All designs seen were exploratory and not confirmed for use in the final design.

## 4.0 Development and Iterations - Synthesis

Design development was broken down into 4 separate sections: steering, motor drive, the whegs, and the main chassis. Once the details of these sections had been established through iteration, the complete design was assembled and iterated to ensure that the functionality that all the sections had separately was retained once they were working cohesively.

### 4.1 Steering

Due to the focus on steering, the design of the mechanism to turn the whegs was prioritised. The goal was to create a system that allowed the body of the robot to turn in as tight a circle as possible. The shape and orientation of the mechanism would also influence the design of the main body and whegs, so was looked into first.

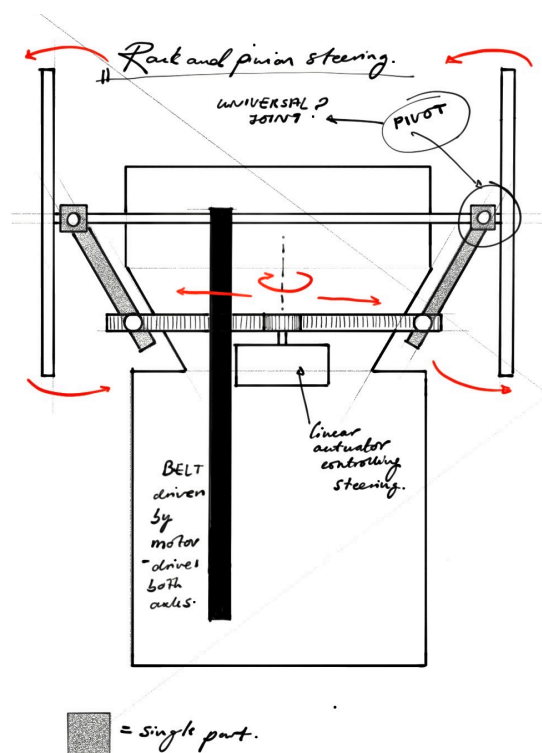


**Figure 7.** Diagram showing how the rack and pinion steering method could be implemented on a MiniWheg.

Inspiration was taken from the steering mechanism used in most modern cars<sup>5</sup> - rack and pinion steering. In a car, turning the steering wheel will turn a pinion which is connected to a rack. The rack moves linearly and pushes the wheels in the direction that the rack is moving. This simple method turns rotational motion from the steering wheel into linear motion on the rack, which is then turned back into rotational motion (for the wheels) via a universal joint. This method was chosen because it is compact and delivers accurate steering.

The need for a universal joint to connect the rack mechanism to the wheg was identified. Research was done into how they work and are implemented<sup>6</sup>. The joint was sketched out so that it could be properly understood, and deemed viable for use in this project.

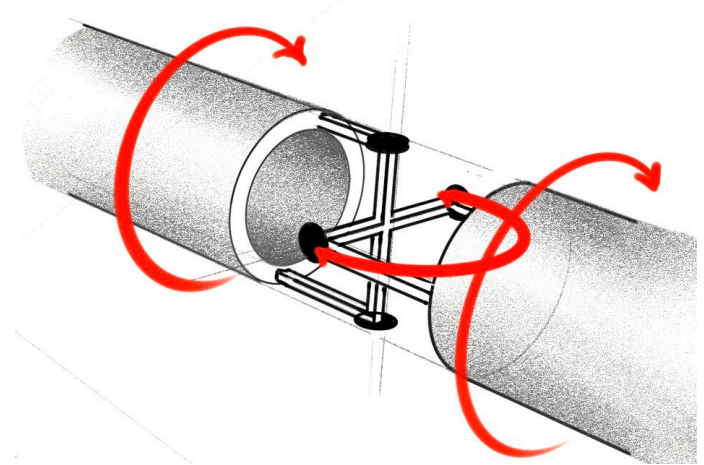
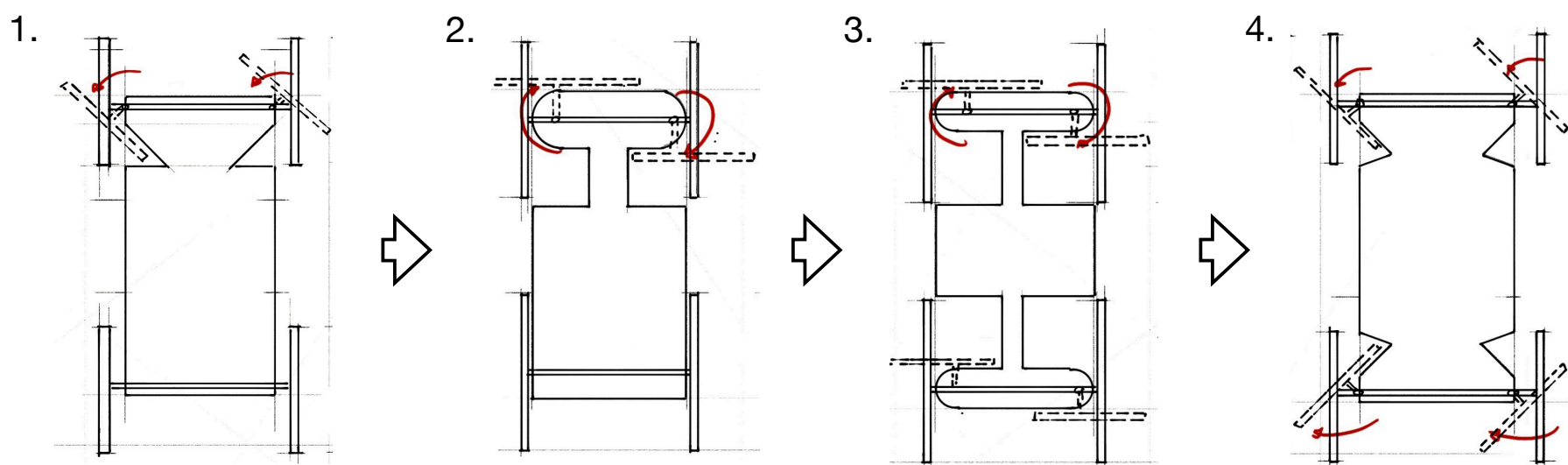


**Figure 8.** Sketch of universal joint.

The rack and pinion method delivers accurate steering, but does not allow for a reduced turning circle. Ideas were brainstormed (shown below) to create a turning system that creates a small turning circle, without reducing the mobility and functionality of the robot. Issues with each iteration listed below, with the final iteration displayed with the reason it was chosen.



- Angle turned by whegs not maximised.

- Rear whegs are not contributing to turning.

- Mechanism impossible to implement

- Rear whegs contributing, using 2 connected rack and pinion systems.

N.B. All iterative drawings are not to scale.



Having decided on a general method of steering, mechanisms to implement the method were explored. Both the front and rear whegs had to be turned using the same servo motor, due to limited space within the robot body, so a system of gears was designed to transfer the turning motion of the servo to the front and rear simultaneously.

### 4.1.1 Servo and Gears

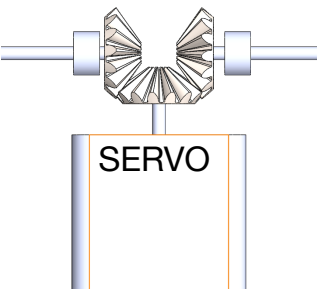


**Figure 9.** Servo and gears

The first aspect of the steering mechanism to be considered was the servo motor used. Even the smallest, least powerful of servo motors provide much more torque than required, so size reduction could be prioritised. The HS-40 Servo, sold by SERVOCITY<sup>7</sup> was selected under this premise. The relevant specifications for this servo are outlined in table 2.

Dimensions	20 x 8.6 x 17 mm
Weight	4.8 g
Voltage range	4.8 - 6.0 V
Output shaft style	15 tooth (A1) spline
No load speed	1.39 rpm

**Table 2.** Servo specifications<sup>7</sup>.

The gears shown in Figure 9 are straight bevel gears: all 3 have 14 teeth and a module of 0.7 as they are being used for power transmission and redirection (as opposed to torque or speed change). These gears allow the rotation of the servo motor to be transmitted to the front and rear of the MiniWheg.

### 4.1.2 Rack and Pinion

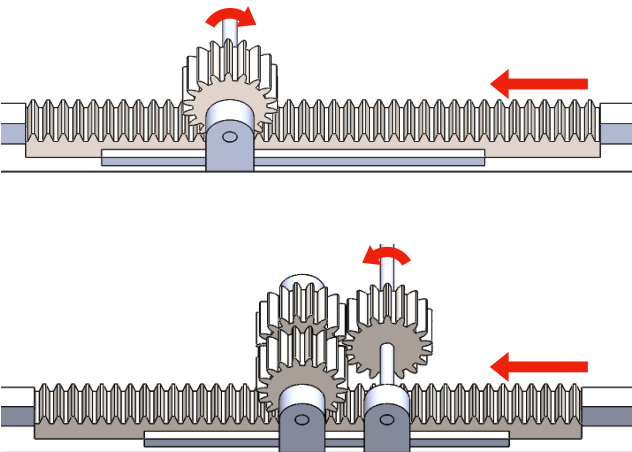


**Figure 10.** First iteration of the rack and pinion at front (above) and rear

Shown in Figure 10 is the first iteration of the rack and pinion system I designed to turn both front and rear whegs simultaneously in a way that would minimise the turning circle. The rear rack and pinion required an extra gear in order to allow both racks to move in the same direction, controlled by the single servo motor. The rack rail and the axle

fixtures were designed specifically for this system. Figure 11 shows the universal joint, and the linkage system that was specifically designed and iterated for this system.

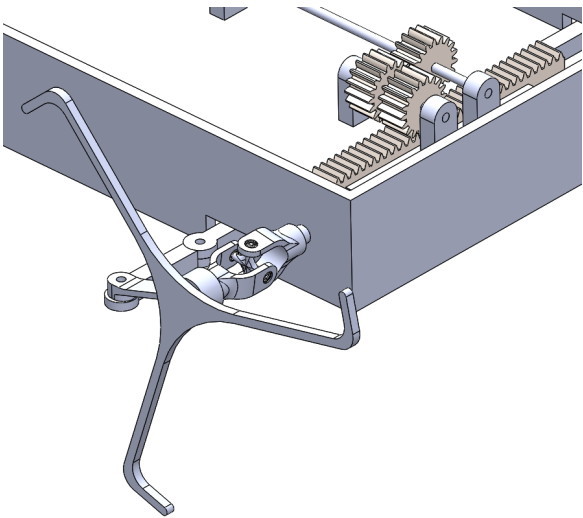


**Figure 11.** Universal joint and linkage system for connection to the rack and pinion.

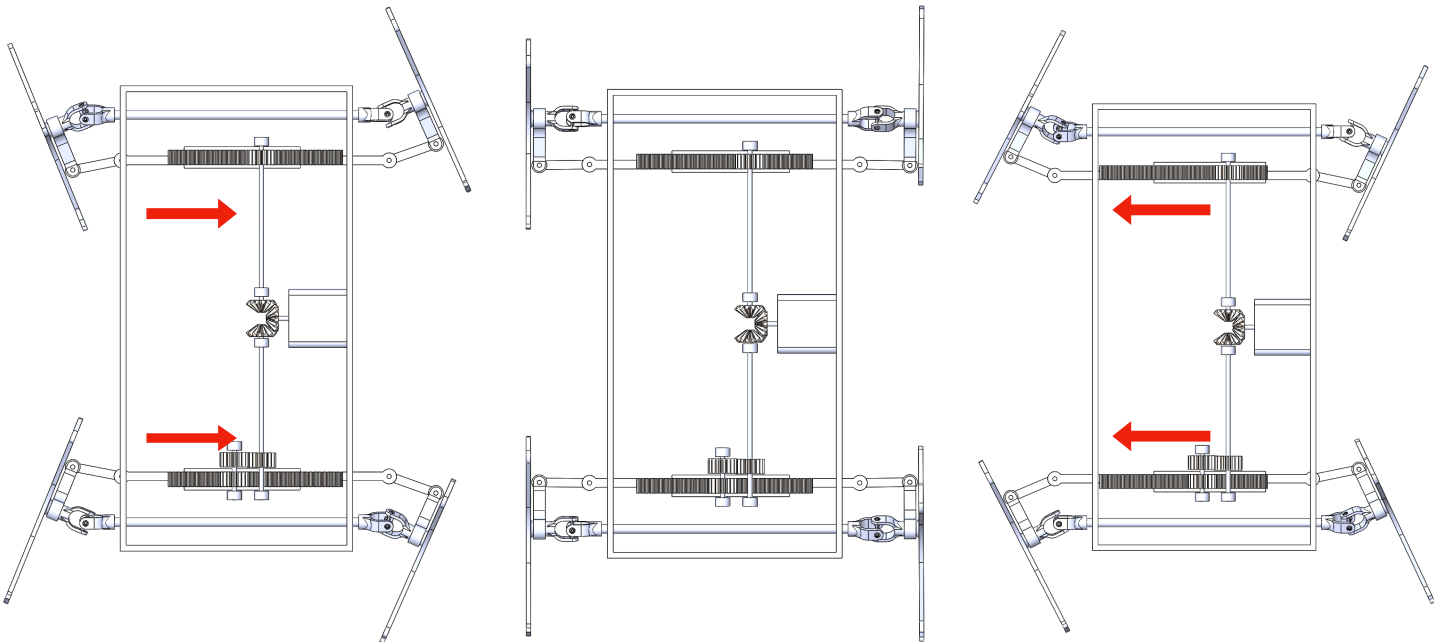


**Figure 12.** Overview of turning mechanism, showing the simultaneous rotation of the front and rear whegs.

Although this was the first iteration of the turning system, it worked well in isolation (without any other parts). The dimensions were edited throughout the process as other parts were added, but the basic mechanism remained unchanged.

## 4.2 Motor drive

When designing the motor drive system for this robot the priorities were: power delivery, consistent speed between whegs, and reaching the speed parameter outlined in the brief.

### 4.2.1 Motor

After considering the types of motor, a brushed DC motor was selected for its low cost and simple motor control.

The following calculations were done to determine the power required from the motor, so that a specific brushed DC motor could be selected from the current market. The calculations (and the values within them) assume that the maximum torque would be required when the robot is climbing an obstacle.

First, the tractive force was calculated:

$$\begin{aligned} F &= mg \\ W &= Fd \\ W &= mgh \end{aligned} \quad \begin{aligned} &\text{Therefore, in terms of} \\ &\text{wheg diameter and} \\ &\text{obstacle height,} \\ &\text{tractive force } F \text{ can} \\ &\text{be expressed as:} \end{aligned} \quad F = \frac{W}{d} = \frac{mgh}{d} = \frac{mg\sqrt{(Dh) - h^2}}{\frac{D}{2} - h}$$

From the tractive force, the required torque and power could be calculated according to the following equations:

$$T = \frac{FDmg}{4} \quad \omega = \frac{v}{r} \quad P = T\omega$$



**Figure 13.** The 17DCT Athlonix 216P 26G2 Brushed DC motor<sup>8</sup>

It was calculated that if the whegs were 40 mm, 2.379 W was required. A safety factor of 1.5 was applied, and this power was too high. If the whegs were 38 mm, 1.827 W was required. After applying the safety factor, the power was 2.741 W, requiring motor with an output of 3W.

$$P = 2.741 \text{ W}$$

The 17DCT Athlonix 216P 26G2 Brushed DC motor was selected, displayed left. This motor, and the servo motor used in the steering mechanism were powered by 4 AAA batteries.

### 4.2.2 Gear box

A gear box was designed to translate the speed of the motor into the speed required by the brief. The required speed was set to 5m/s (far above the specification), so that the robot had the capability of moving at 10x the required speed.

Input speed of motor: 7657 rpm = **801.84 rad/s**

Output speed = 5 m/s = **131.58 rad/s**

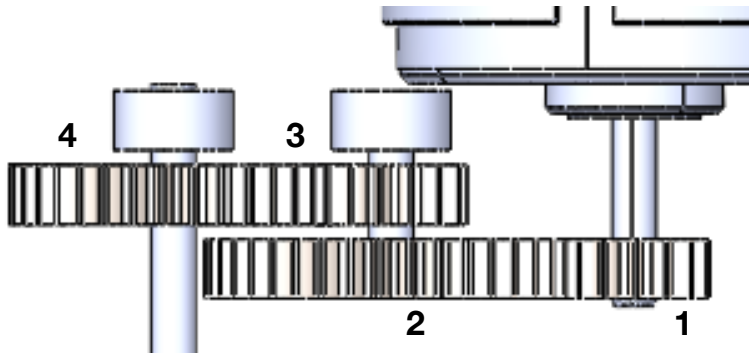
Transmission ratio = 801.84/131.58 = **6.093**

The transmission ratio demanded the use of a gear box, as it is one of the few types of transmission that can manage such a large ratio.

A gear train was created using the following equation:

$$n_2 = \left| \frac{N_1}{N_2} n_1 \right| = \left| \frac{d_1}{d_2} n_1 \right|$$

Where  $n$  is the speed of the gear, and  $N$  is the number of teeth on that gear.



The speed reduction had to be done in two steps:

$N_1 = 15$	$n_1 = 801.84 \text{ rpm}$
$N_2 = 40$	$n_2 = 300.69 \text{ rpm}$
$N_3 = 15$	$n_3 = 300.69 \text{ rpm}$
$N_4 = 35$	$n_4 = \mathbf{128.86 \text{ rpm}}$

**128.86 rpm  $\approx$  131.58 rpm**

**Figure 14.** Gear train to reduce the output speed.

All gears had a module of 0.3

### 4.2.3 Power transmission

In order to maximise the delivery of power from the motor to the ground, a 4 wheel drive system was designed for the robot by driving both the axles with 1 motor.

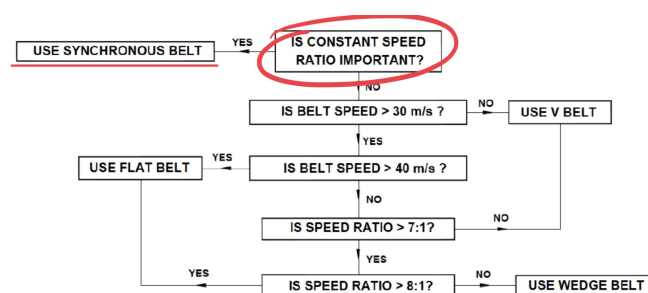


**Figure 15.** Belt selection tree

Initially, a chain drive was considered as chain drives are capable of delivering high torque and speed. However, due to the expense and lubrication difficulties associated with chain drives, a belt drive was chosen to drive the whegs. Using the belt selection tree, it was immediately apparent that a synchronous belt would be most ideal, as a constant speed ratio between both axles and the motor is important for this robot.

The optimal belt was selected using the method as outlined in the CONTI HTD Manual Catalogue. However, there was no difference in the diameter of the driving and driven belt pulley, as the speed reduction is achieved by the gear box. For this reason, many of the values used to determine the specification for the HTD belt were redundant. Therefore the belt length required was calculated from the values below.

$$\begin{aligned} c_2 &= 1.2 & z_g &= z_w = 22 \text{ teeth} \\ c_3 &= 0 & d_{wk} &= d_{wg} = 11.89 \text{ mm} \\ c_4 &= 0.2 & i &= 1 \end{aligned}$$

Length of belt required = **244 mm**

An outside idler pulley belt tensioner was used take up potential slack in the belt and to improve drive performance.

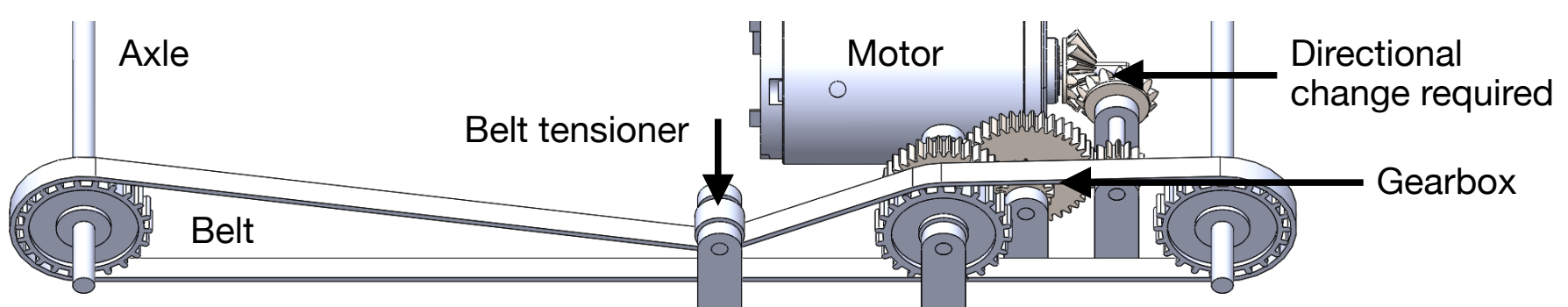


**Figure 15.** Complete motor drive system



## 4.3 Whegs

As determined in the research, the arrangement of 3 evenly spaced spokes was the optimal shape for the whegs with each separate wveg offset at 60 degrees - this increases contact with the surface the robot is moving over.

### 4.3.1 Shape Iterations

Due to this preset having been previously ascertained, the design of the whegs of this robot was led initially by mechanical requirements, and then was optimised through simulation analysis: looking at static, frequency and fatigue simulation results to determine where the wveg requires attention or redesign. This process is shown in more detail in Engineering analysis.

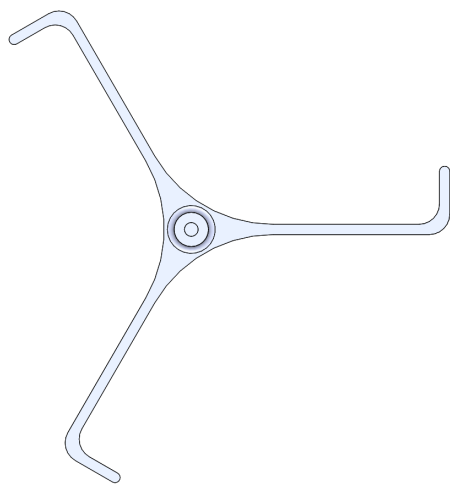


**Figure 16.** Wheg iteration 1

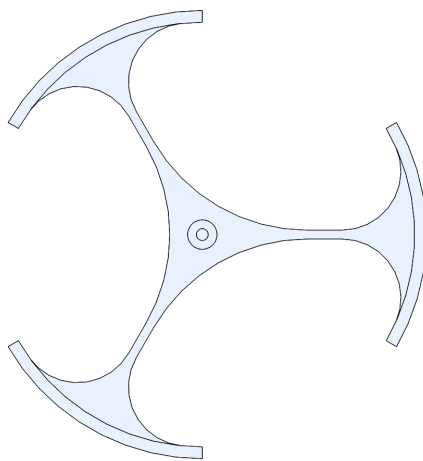


**Figure 17.** Wheg iteration 2

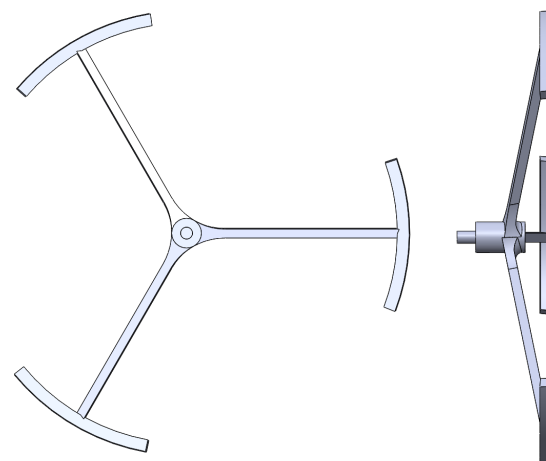


**Figure 18.** Wheg iteration 3, displaying conical configuration

Iteration 1 (Figure 16) prioritised the space between each wveg, as this helps the robot to climb obstacles, but it was quickly realised that this formation would mean that if the robot was flipped over, the whegs would only be effective moving backwards. This is taken into account in iteration 2 (Figure 17), where the leg is reversible. Iteration 3 (Figure 18) employs the reversible leg and also explores having the wveg rotate about a 3D cone instead of a circle, which would allow for a further decrease in turning circle. The initial leg length was 38 mm (specified in Section 4.2.1 as a requirement for motor power) but was increase to 38.6 mm after iteration. Further iterations are discussed in the engineering analysis of the wveg.

## 4.4 Main body - Shell

The main body is responsible for keeping the internal mechanisms and components from damage, whilst also allowing access for repair and battery change. The following section details how the final shell design was formulated from these requirements.

### 4.4.1 Shape Iterations

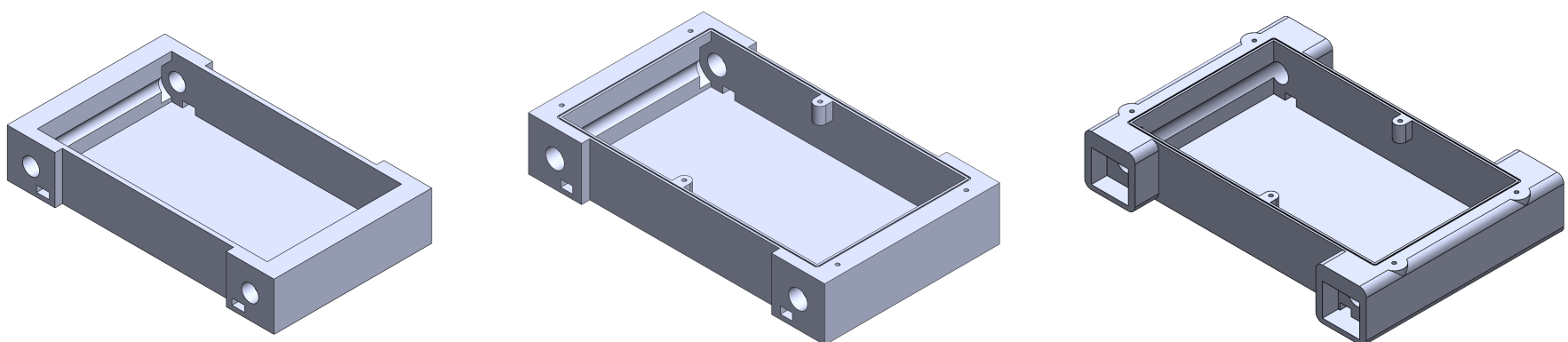


**Figure 19.** Progressive iterations of shell design - the initial design provided the bare minimum to house the components, and was developed to provide Ingress Protection IP 53

#### 4.4.2 Ingress Protection

As specified by the brief, the Ingress Protection required for this robot is IP 53. According to the international standard IEC 60529, Ingress Protection 'classifies the degrees of protection provided against the intrusion of solid objects (including body parts like hands and fingers), dust, accidental contact, and water in electrical enclosures'<sup>9</sup>. Specifically, IP 53 requires that dust ingress must not occur in sufficient quantity to interfere with the satisfactory operation of the equipment, and water falling as a spray at any angle up to 60° from the vertical shall have no harmful effect.

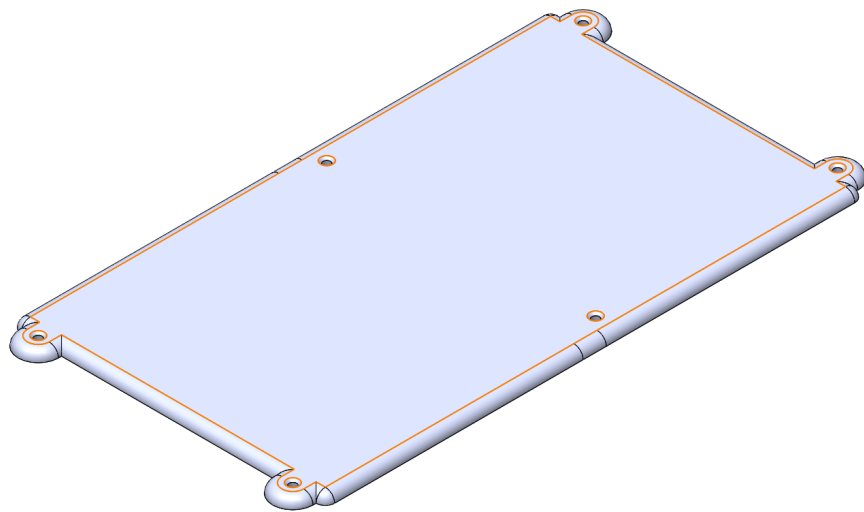


**Figure 20.** Lid designed to be screwed in 6 places, with indents for screw heads

An O-ring seal groove was added to the perimeter of the shell, so that when the lid was screwed on, the components are protected from water and dust completely from above. The bearings that hold the axle prevent water and dust entering the robot through the axle holes, up to the requirement of IP 53.

In order to access the battery for changing the cells, and to access the components for repair, the top lid was designed to be removable using screws (Figure 20). The lid was designed to be screwed in 6 separate places, to ensure maximum security, and screw indents were designed so that the screws were almost flush with the surface.

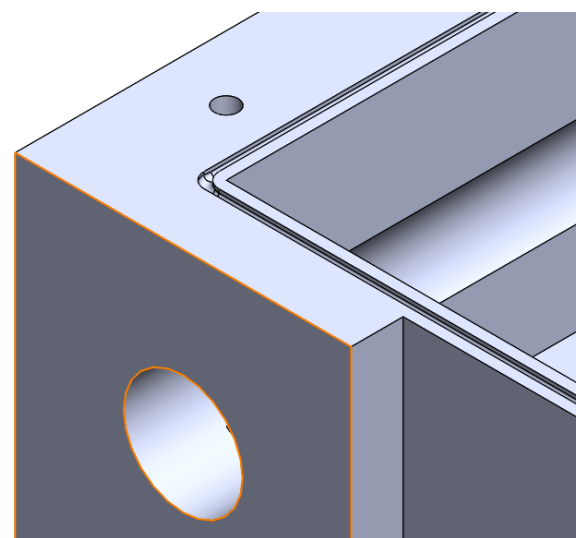


**Figure 21.** O-ring seal groove running the full perimeter of the robot body

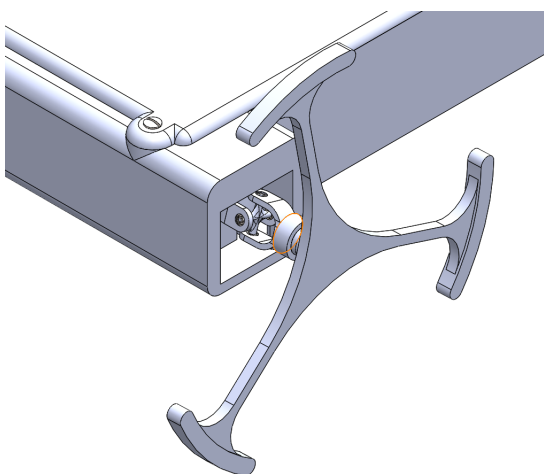


**Figure 22.** Sheaths built into the shell for minor protection of Universal Joint mechanism from dust and splashes of water

Ingress Protection for the sections of the steering mechanism were difficult due to the number of moving parts. In reality, a dynamic seal would need to be prototyped and applied to achieve full water protection, but a sheath built into the shell provides protection for the mechanism from dust ingress and light splashes of water (Figure 22). To ensure the shell would survive a drop height of 300 mm (specified by the brief), the thinnest section of the shell is 2 mm, providing enough structural strength throughout in combination with the structural strength of the wheels (outlined in detail in Engineering analysis).

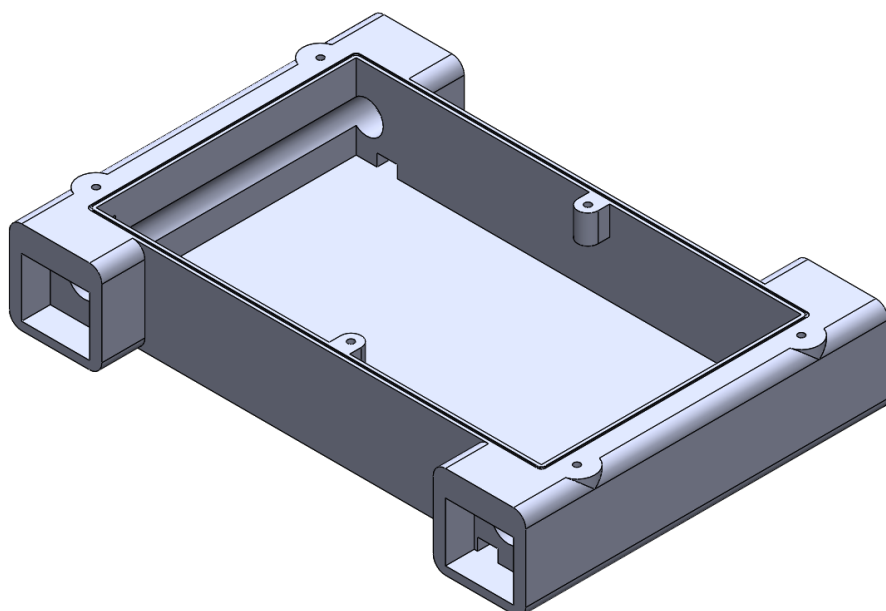


**Figure 23.** Final shell iteration

## 5.0 Engineering Analysis - Analysis

### 5.1 Wheg

The simulation was run with parameters that would test the wheg in a situation in which it would undergo the maximum forces it is required to withstand: a drop from 300 mm. The force that the wheg would undergo if the robot fell on one leg from a height of 300 mm was calculated using the SUVAT and momentum equations below:

$$v^2 = u^2 + 2gs \quad F = \frac{m(v - u)}{dt}$$

The mass of the robot was set as 0.4 kg (maximum mass of the components + maximum payload). Velocity at which the wheg hits the ground  $v$  was calculated to be 2.426 m/s and the time taken for the robot to decelerate to a stop was estimated to be 0.1s. Therefore the maximum force acting on the leg during deceleration to a stop was calculated to be **9.704 N**.

The third iteration shown in Figure 18 failed at 2 N, with a displacement of 5.6 mm as shown in Figure 24. This failure was due to the conical configuration that was implemented to increase the turning circle, but as this compromised the structural integrity of the wheg, a design that combined iteration 2 and 3 was created, without the conical configuration.

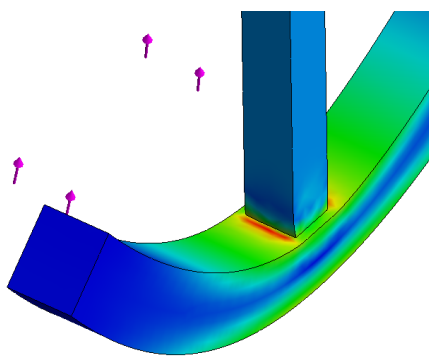


**Figure 25.** Wheg iteration 4 stress concentration at end of wheg.

The next iteration survived had a displacement of 6.9 mm at the target force of 9.704 N as shown in Figure 25. This improvement was due to the force being absorbed by the vertical leg, rather than stress being focussed on the thinnest part of the wheg. However stress concentration meant that the maximum MPa was high - this was amended by thickening the legs from 1.5 mm to 2 mm and by using fillets to disperse the stress concentrators, as shown in Figure 26. The final wheg iteration withstood the full 9.704 N with only 0.46 mm of displacement, and therefore would not fail under the parameters of the brief. However, after a number of life cycles, the wheg would fail by fracture.

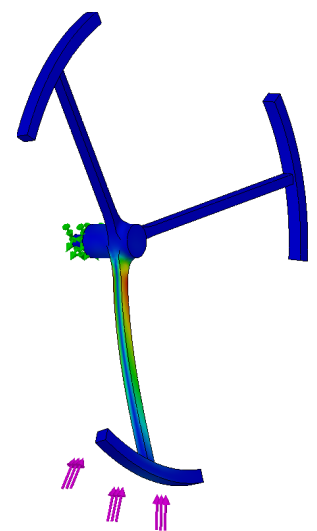


**Figure 24.** Wheg iteration 3 failure due to stress concentration on leg.

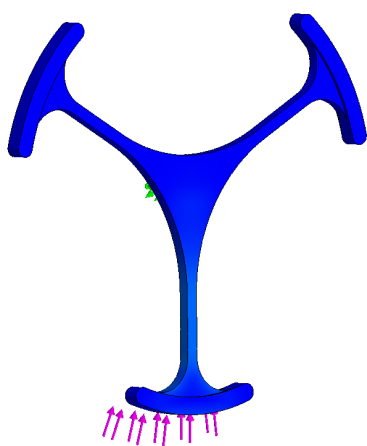


**Figure 26.** Final wheg iteration static simulation - little to no stress

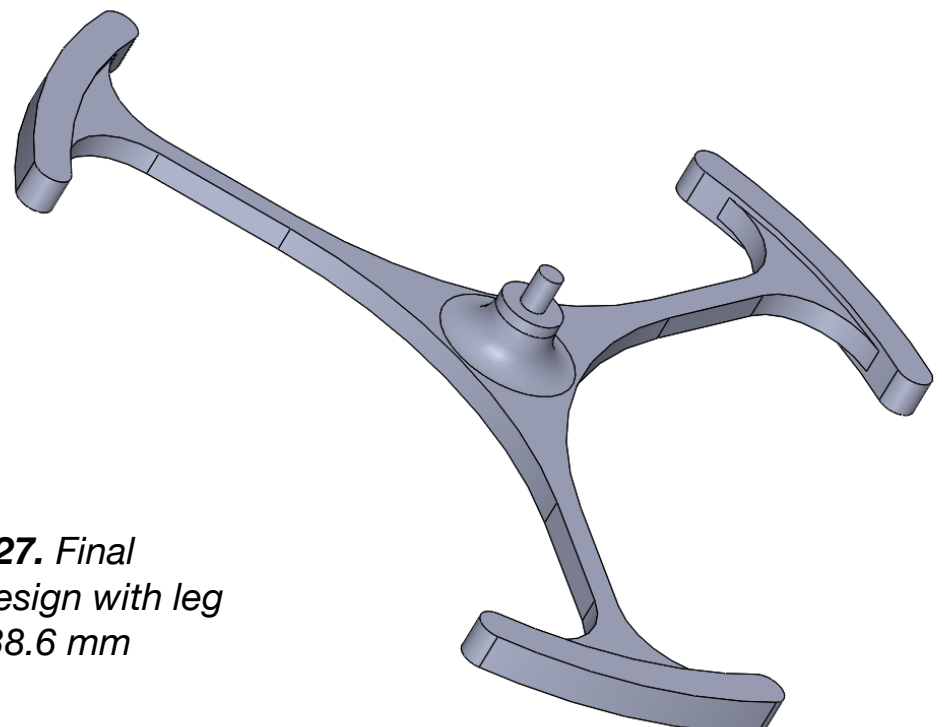
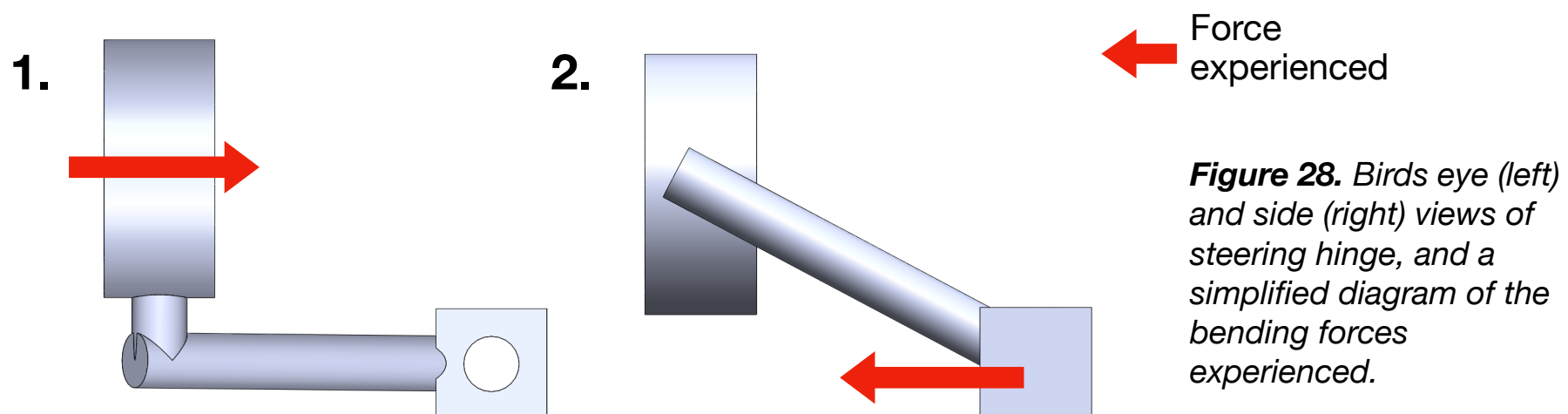


**Figure 27.** Final wheg design with leg length 38.6 mm

## 5.2 Steering Hinge

The steering hinge was designed especially for this robot to work in the steering mechanism. It experiences a number of bending forces due to its shape and function which can be simplified to two static simulation scenarios, as shown in Figure 28.



It was determined that this part would fail under excessive bending due to its function, and so simulations were run and iterations made to mitigate against this. The maximum forces that the steering hinge would undergo were explored due to the set up of the simulation - the hinge in the cube was set as a fixed geometry to mimic a situation in which the whole mechanism became jammed. Initially, 5N of force was applied to the axle sheath to highlight where the part would fail. Stress concentrated in the joints between the shaft and the hinges (Figure 29).

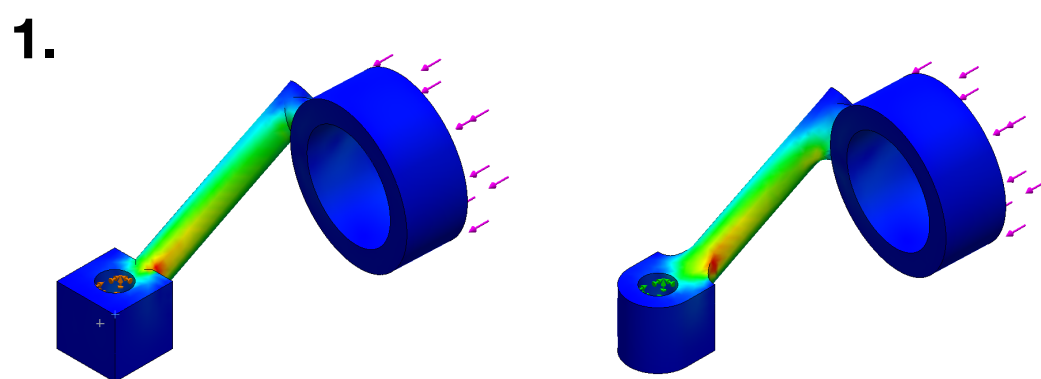


**Figure 29.** Stress at a maximum at where the shaft connects the hinges.

After the first simulation, the steering hinge was optimised to reduce the stress concentrators that formed as a result of these specific bending forces as much as possible. The displacement in the simulations was reduced from 9.41 mm to 8.33 mm. This is still overly large, and so more iterations need to be explored to improve the security of this part.

In scenario 2, the locations of the fixed geometry and force were swapped to explore a different situation. This scenario highlighted a bending in the main shaft, which was mitigated by increasing the diameter of the shaft, as shown in Figure 30. This change, in combination with some more filleting, reduced the stress and displacement of both scenarios. With 5 N of force in both situations, the displacement was 2.89 mm in scenario one, and 1.492 mm in scenario two, a vast improvement. However, these simulations represent simplifications in the mechanism, and so will not be entirely accurate - for this reason, real-life prototyping would have to be conducted to ensure the security of this part.

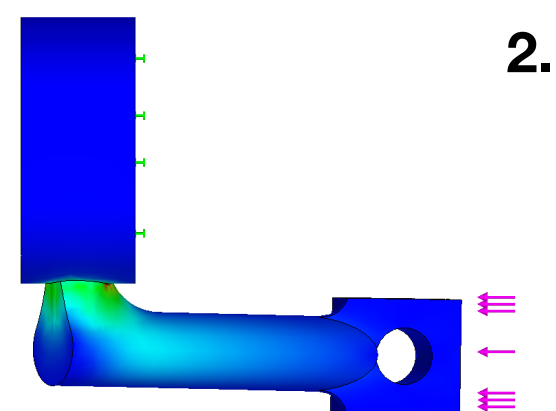


**Figure 30.** Further improvements due to situation 2

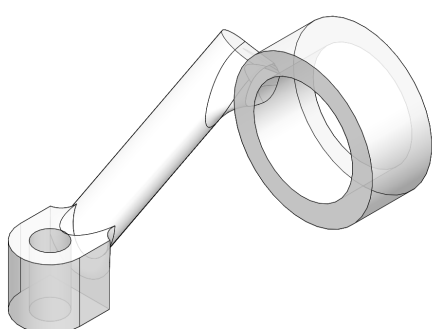


**Figure 31.** Final design of steering hinge, displayed polycarbonate - the material used and simulated.



# Final Design

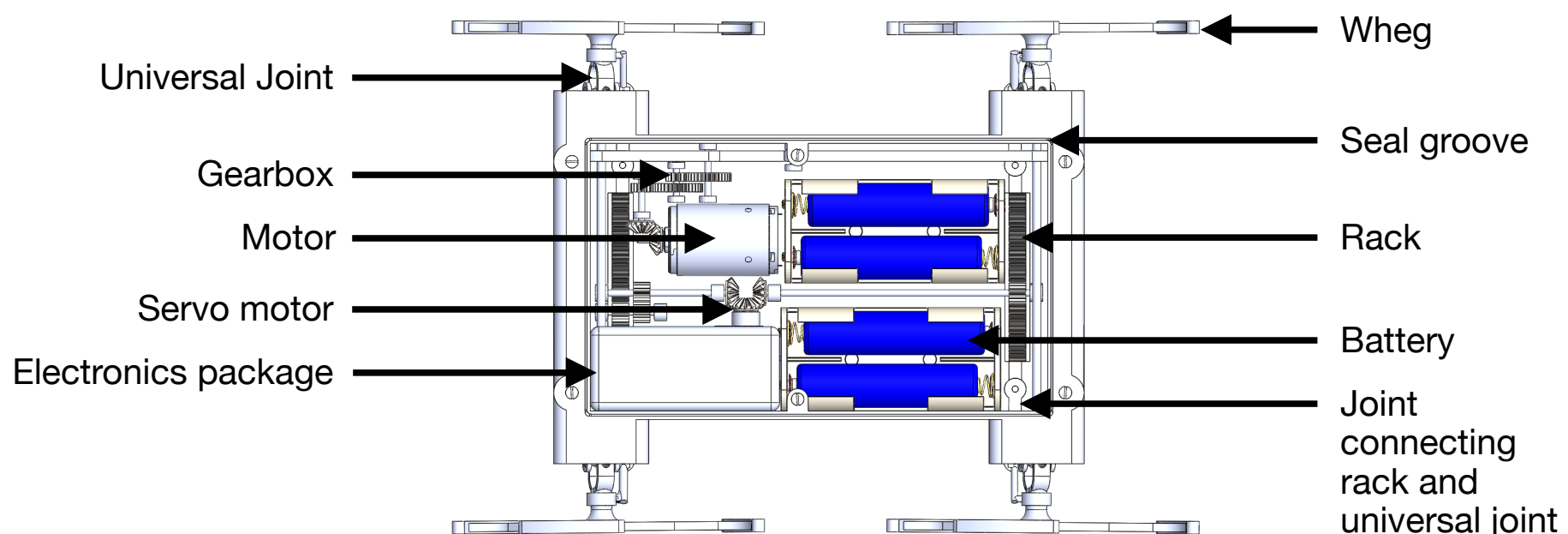


**Figure 32.** Final design from bird's eye

The final design weighed 154.76 grams, which is almost a quarter less than the specified weight. This means that the robot has improved agility on rough terrain, allowing it to complete its tasks with more efficiency. The cost of the robot was below £200 - the motor and servo were the most expensive components with a combined cost of £12.57, with all other expenses consisting of the value of the material used for the specially designed parts - a combination of PC and stainless steel.

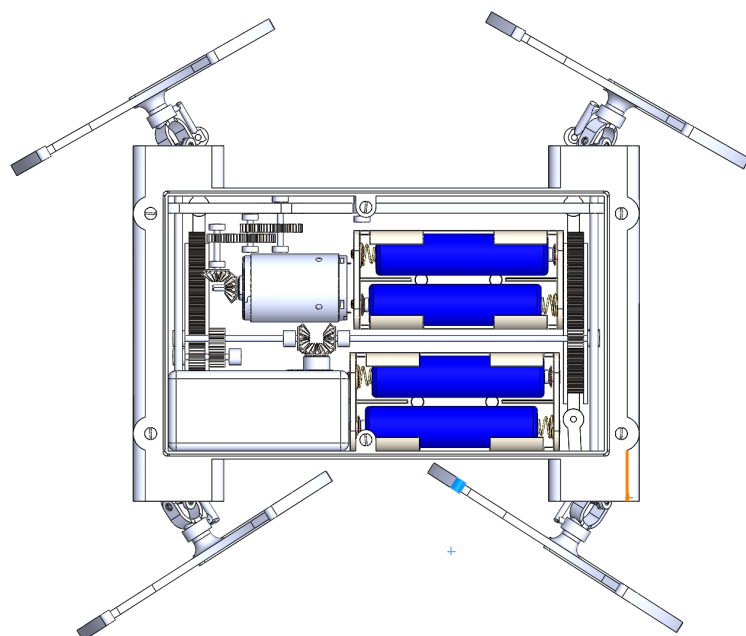


**Figure 33.** Demonstration of maximum steering

The steering mechanism designed for this robot allowed for a turning circle of 122.55 mm (shown by Figure 33) - a 23.41% reduction from the brief specification. This is possible due to both pairs of wheels being able to turn 25° inwards and outwards and the reduced length of the robot, with a distance of 103.58 mm between axles. This allows the robot to access smaller spaces and have improved agility when traversing rough terrain.

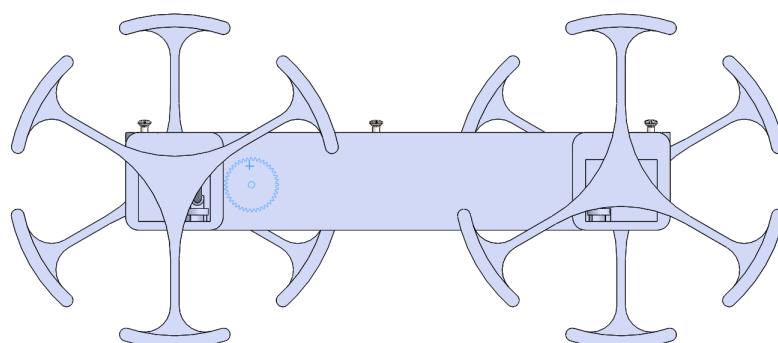


**Figure 34.** The wheels were positioned 60° out of phase to maximise contact with the ground

Width of chassis	88.50 mm
Length of chassis	126.12 mm
Total mass	154.76 g
BoM cost	< £200
Leg length	38.60 mm
Obstacle height	55 mm
Turning circle radius	122.55 mm

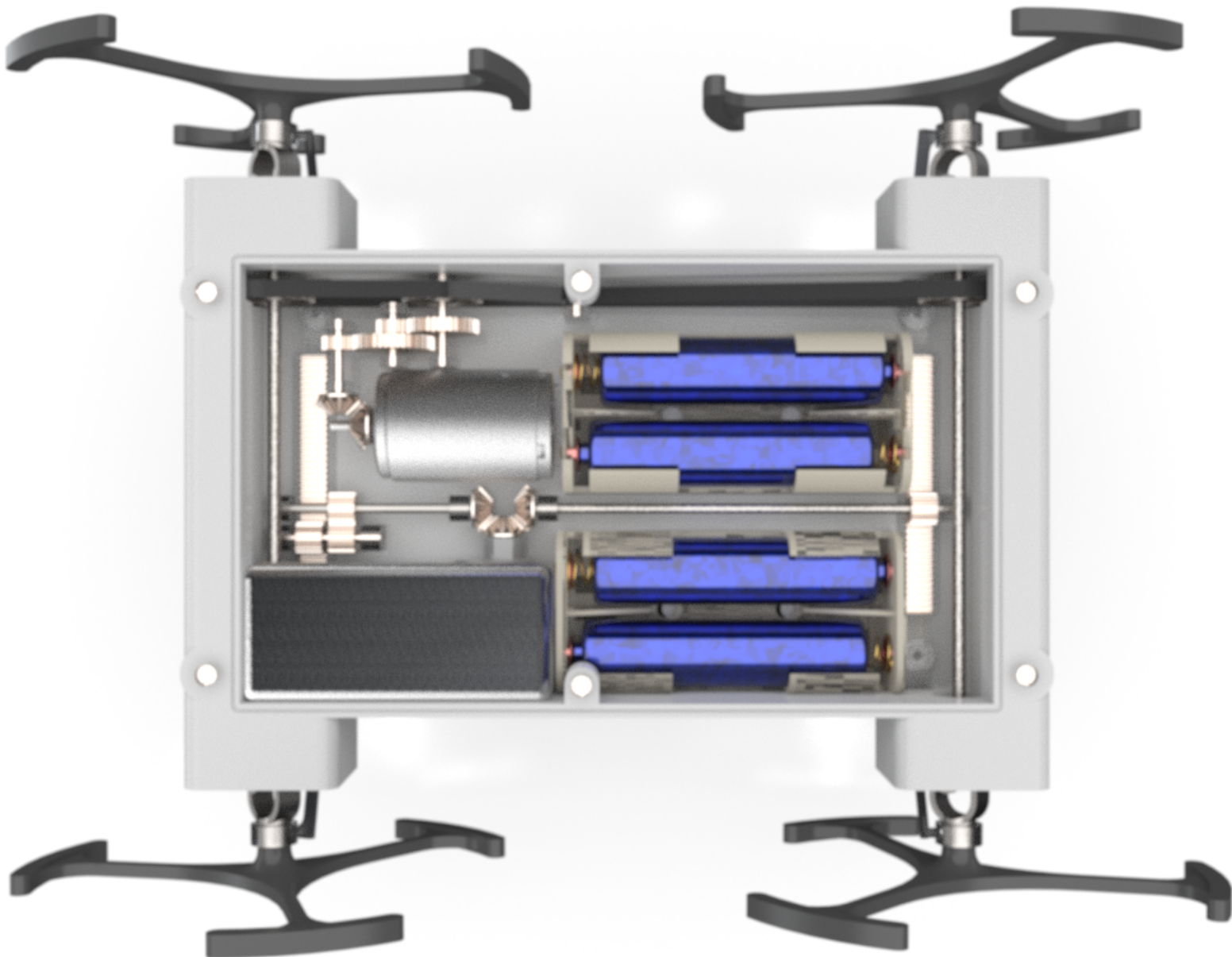
**Table 3.** Parameters of final robot design

The width had to exceed the value stated by the brief to allow for the Universal Joint mechanism to extend far enough from the main chassis, permitting all wheels to turn a full 50° - 25° in each direction.

The general assembly drawing, as well as 3 part drawings are included at the end of this document. The full Solidworks model can be found using the following link: <https://imperialcollegelondon.app.box.com/folder/111560522317>



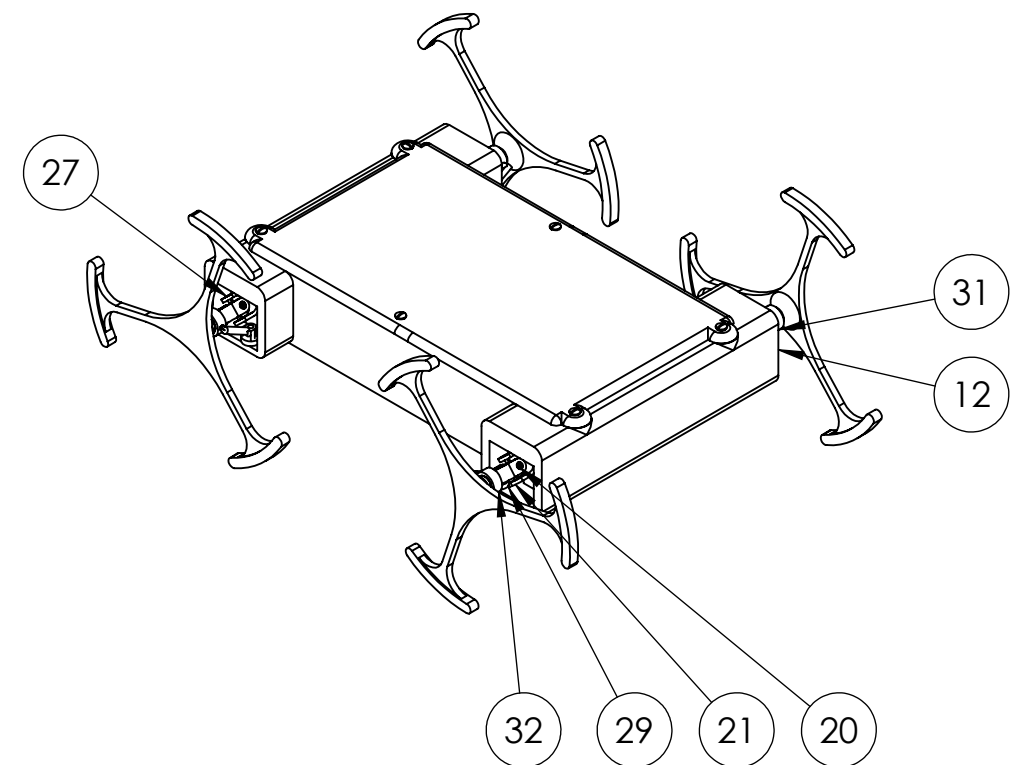
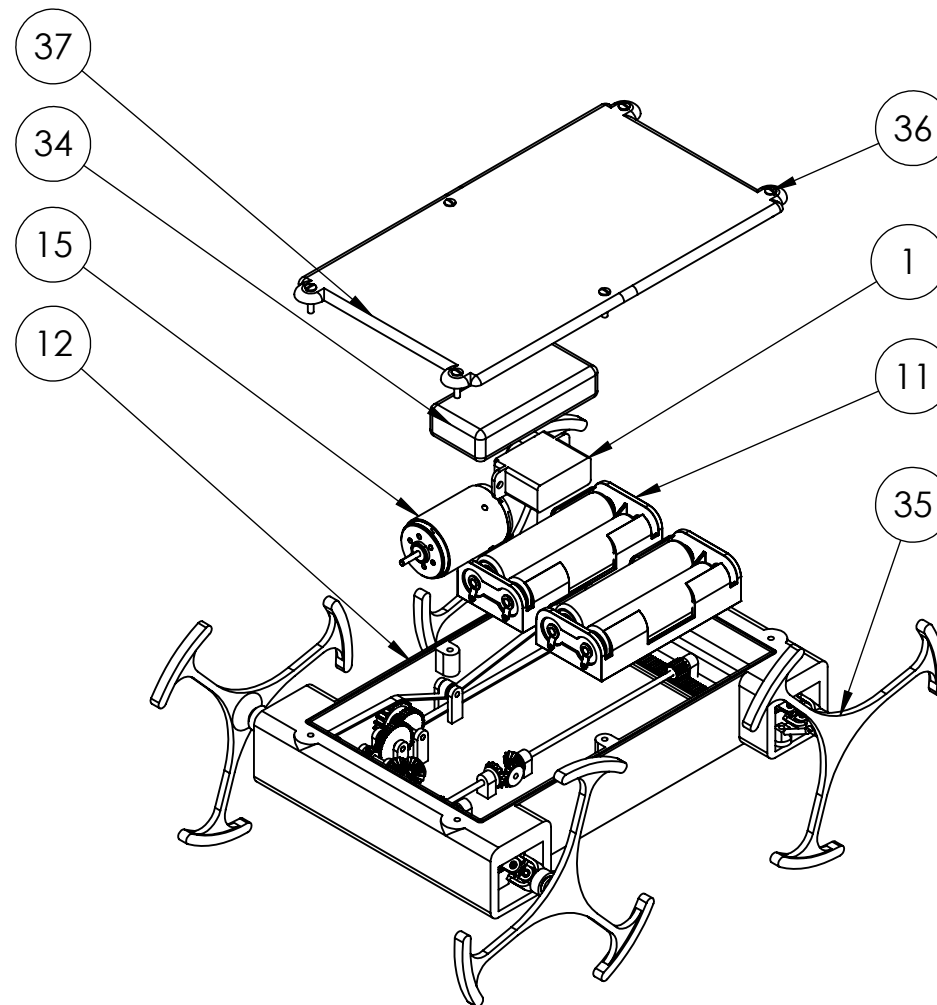
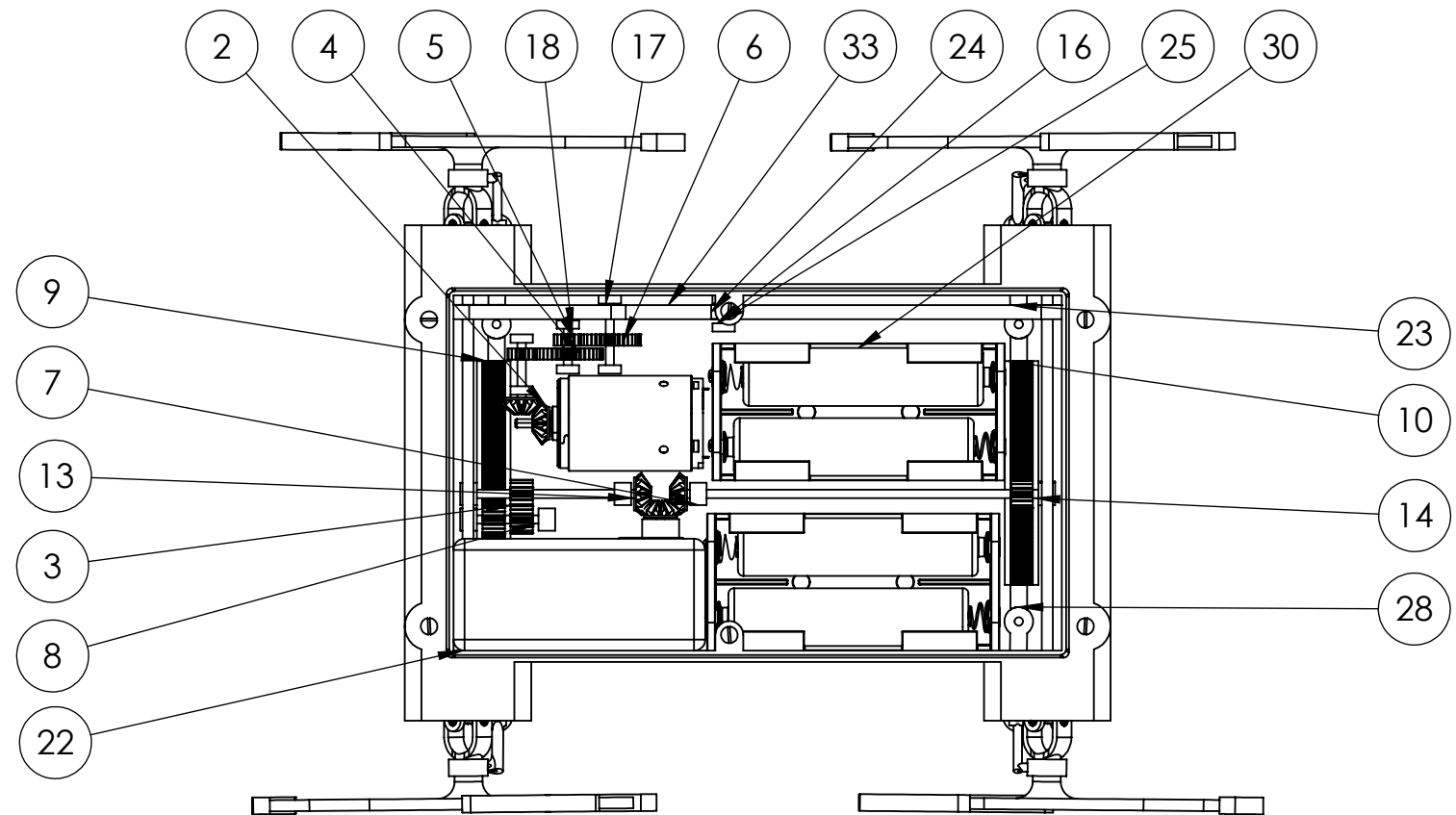
7.0 Renders



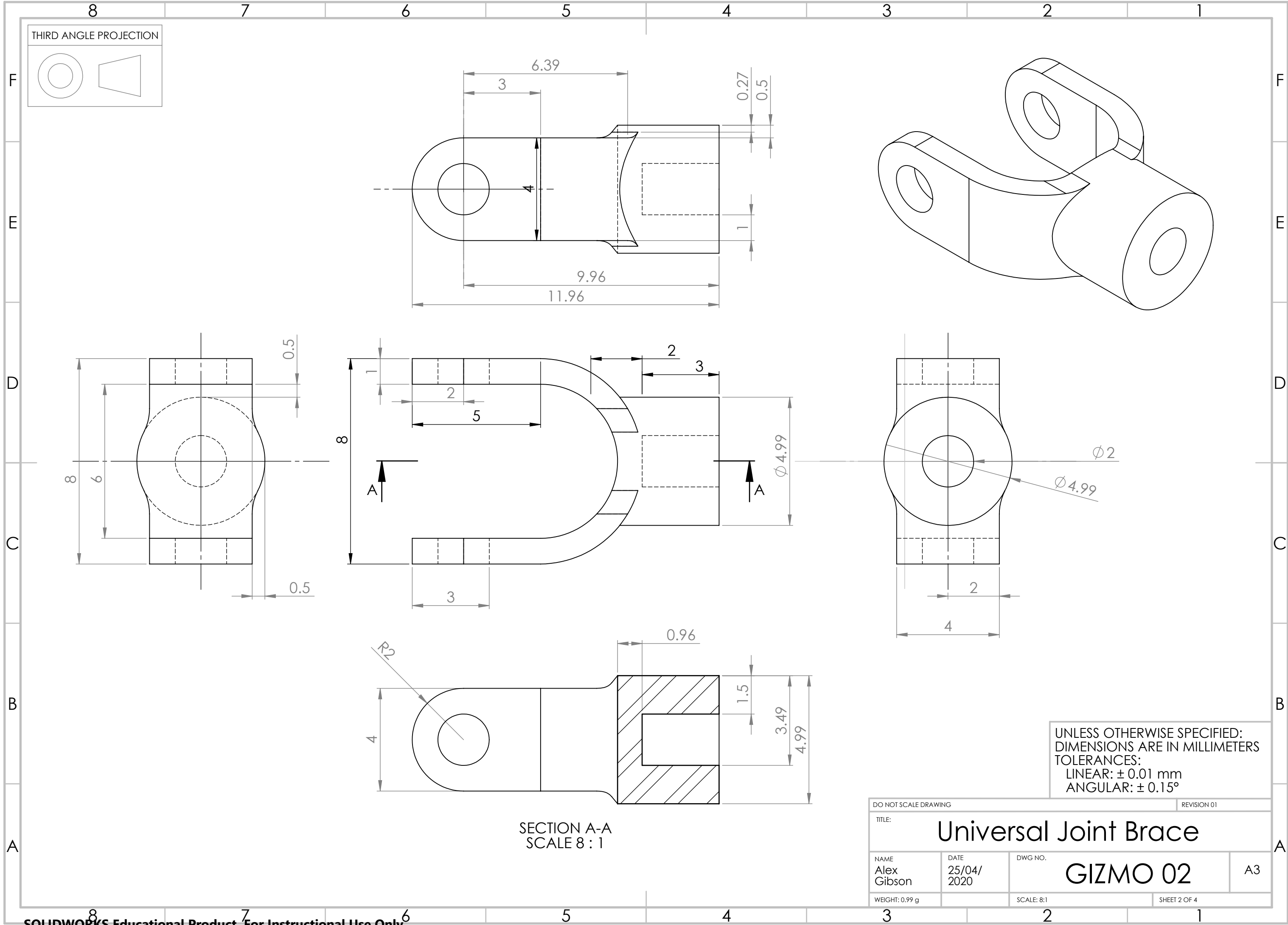
## 8.0 References:

1. Morrey J, Lambrecht B, Horschler A, Ritzmann R, Quinn R. Highly Mobile and Robust Small Quadraped Robots [Internet]. 2003 [cited 8 April 2020]. Available from: [https://www.researchgate.net/profile/Andrew\\_Horschler/publication/4046245\\_Highly\\_mobile\\_and\\_robust\\_small\\_quadraped\\_robots/links/00b4953cd3245bb9a9000000/Highly-mobile-and-robust-small-quadraped-robots.pdf](https://www.researchgate.net/profile/Andrew_Horschler/publication/4046245_Highly_mobile_and_robust_small_quadraped_robots/links/00b4953cd3245bb9a9000000/Highly-mobile-and-robust-small-quadraped-robots.pdf)
2. Eich M, Grimminger F, Bosse S, Spennberg D, Kirchner F. Asguard : A Hybrid-Wheel Security and SAR-Robot Using Bio-Inspired Locomotion for Rough Terrain [Internet]. Semantic Scholar. 2020 [cited 8 April 2020]. Available from: <https://www.semanticscholar.org/paper/Asguard-%3A-A-Hybrid-Wheel-Security-and-SAR-Robot-for-Eich-Grimminger/933f7dd4094fca7db1cf9229fcc651eb38e74b99>
3. Robots Archives | beanz Magazine [Internet]. beanz Magazine. 2020 [cited 8 April 2020]. Available from: <https://www.kidscodex.com/sections/all-stories/robots/>
4. Speedy Whegs Robot Runs at 44 km/h, Can Climb Obstacles - Robotic Gizmos [Internet]. Robotic Gizmos. 2020 [cited 8 April 2020]. Available from: <https://www.roboticgizmos.com/speedy-whegs-robot/>
5. Garden H, HowStuffWorks, Auto, Hood, Suspension. How Car Steering Works [Internet]. HowStuffWorks. 2020 [cited 11 April 2020]. Available from: <https://auto.howstuffworks.com/steering2.htm>
6. What is a Universal Joint? | Machine Service, Inc. [Internet]. Machineservice.com. 2020 [cited 11 April 2020]. Available from: <https://www.machineservice.com/products/universal-joints/what-is-a-universal-joint/>
7. HS-40 Servo [Internet]. Servocity.com. 2020 [cited 17 April 2020]. Available from: <https://www.servocity.com/hitec-hs-40-servo>
8. 17N78 Athlonix Brush DC Motor [Internet]. Portescap.com. 2020 [cited 22 April 2020]. Available from: <https://www.portescap.com/products/brush-dc-motor>
9. IP Rating Chart [Internet]. dsmt.com. 2020 [cited 24 April 2020]. Available from: <http://www.dsmt.com/resources/ip-rating-chart/>

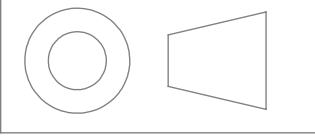
8		7	
	ITEM NO.	PART NUMBER	QTY.
F	1	Servo motor	1
	2	ISO - Straight bevel gear 0.5M 14GT 12PT 20PA 3FW --- 14O75H4MD1.5N	5
	3	ISO - Spur gear 0.3M 15T 20PA 4FW ---S15A75H50L1.5N	4
E	4	ISO - Spur gear 0.3M 40T 20PA 2FW ---S40A75H50L1.5N	1
	5	ISO - Spur gear 0.3M 15T 20PA 2FW ---S15A75H50L1.5N	2
	6	ISO - Spur gear 0.3M 35T 20PA 2FW ---S35A75H50L1.5N	1
	7	Shaft hold	6
	8	Direction change axle	1
D	9	ISO - Rack-spur - rectangular 0.3M 20PA 4FW 2PH 40L---SAll	2
	10	Rack holder	4
	11	Battery	4
	12	Shell	1
	13	Turning axle (rear)	1
	14	Turning axle (front)	1
	15	Motor	1
	16	Shaft hold - gearbox	8
C	17	Gearbox axle	2
	18	Gearbox extension axle	1
	19	ISO 1224 - 170508 - R,18,SI,NC,18_68	4
	20	ISO 1224 - 170602 - R,8,SI,NC,8_68	16
	21	Universal joint brace	8
	22	Main shaft	2
B	23	Synchronous belt gear (main axle)	2
	24	Belt tensioner wheel	1
	25	Belt tensioner axle	1
	26	Synchronous belt gear (gearbox)	1
	27	Universal joint cross	4
	28	Rack joint (attached to rack)	4
A	29	Rack joint	4
	30	AAA cells	4
	31	Steering hinge (L)	2
	32	Steering hinge (R)	2
	33	Belt1-1^GIZMO MINIWHEG ASSEMBLY	1
	34	Electronics package	1
	35	Wheg	4
	36	ISO 2010 - M1.6 x 8 - 8N	6
	37	Lid	1



DO NOT SCALE DRAWING		REVISION 01	
TITLE: <h1>General Assembly Drawing</h1>			
NAME Alex Gibson	DATE 25/04/2020	DWG NO. <h1>GIZMO 01</h1>	A3
WEIGHT: 154.76 g		SCALE:1:5	SHEET 1 OF 4

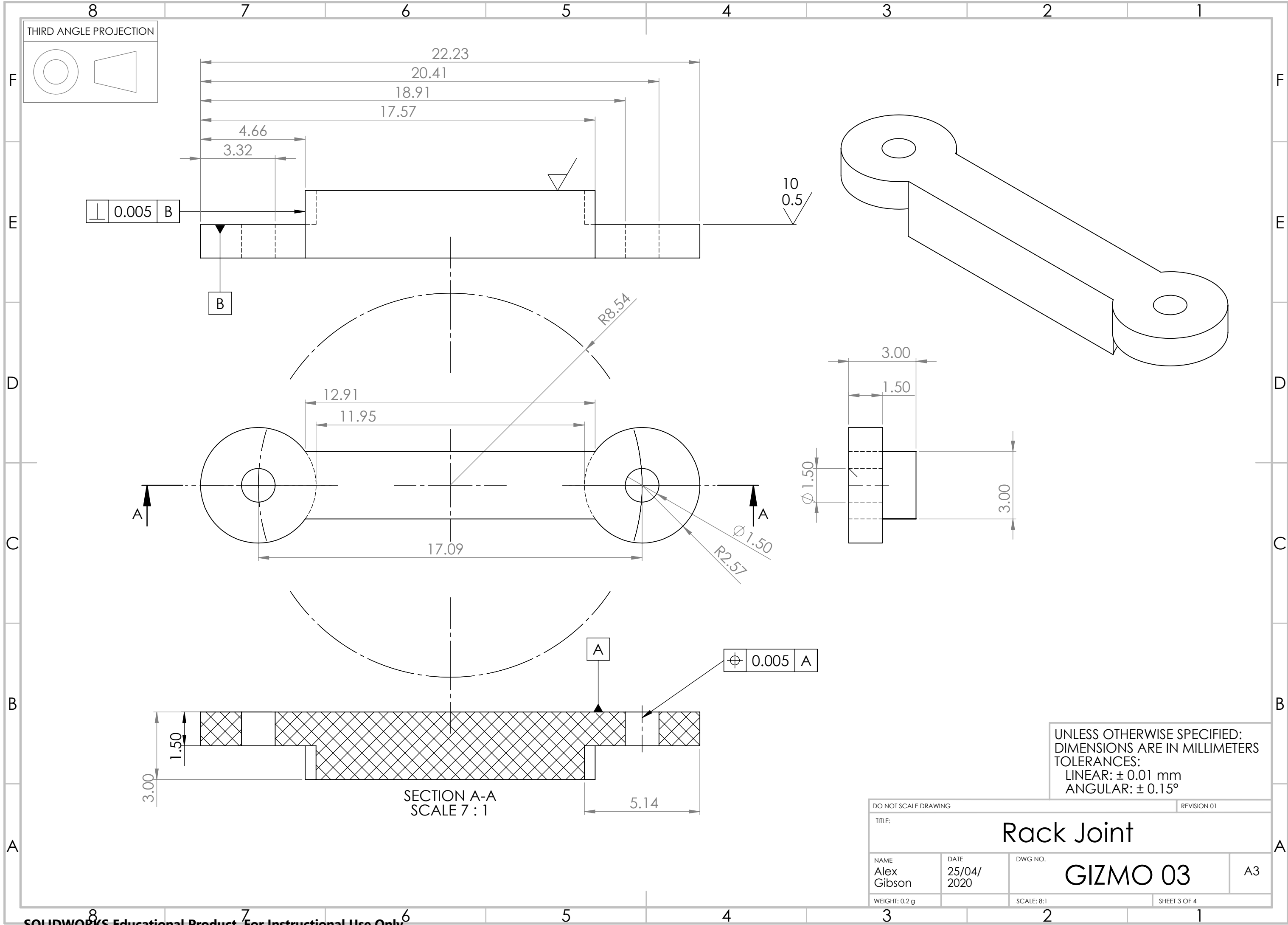


THIRD ANGLE PROJECTION



UNLESS OTHERWISE SPECIFIED:  
DIMENSIONS ARE IN MILLIMETERS  
TOLERANCES:  
LINEAR:  $\pm 0.01$  mm  
ANGULAR:  $\pm 0.15^\circ$

DO NOT SCALE DRAWING			REVISION 01	
TITLE: <div>Universal Joint Brace</div>				
NAME Alex Gibson	DATE 25/04/ 2020	DWG NO. <div>GIZMO 02</div>		A3
WEIGHT: 0.99 g		SCALE: 8:1	SHEET 2 OF 4	



DO NOT SCALE DRAWING			REVISION 01	
TITLE: Rack Joint				
NAME Alex Gibson	DATE 25/04/2020	DWG NO. GIZMO 03		A3
WEIGHT: 0.2 g		SCALE: 8:1	SHEET 3 OF 4	



